



## Contrasting biosphere responses to hydrometeorological extremes: revisiting the 2010 western Russian Heatwave

Milan Flach<sup>1</sup>, Sebastian Sippel<sup>2</sup>, Fabian Gans<sup>1</sup>, Ana Bastos<sup>3</sup>, Alexander Brenning<sup>4,5</sup>, Markus Reichstein<sup>1,5</sup>, and Miguel D. Mahecha<sup>1,5</sup>

<sup>1</sup>Max Planck Institute for Biogeochemistry, Department Biogeochemical Integration, P. O. Box 10 01 64, D-07701 Jena, Germany

<sup>2</sup>Norwegian Institute of Bioeconomy Research, Ås, Norway

<sup>3</sup>Laboratoire des Sciences du Climat et de l'Environnement, LSCE/IPSL, CEA-CNRS-UVSQ, Université Paris-Saclay, 91191 Gif-sur-Yvette, France

<sup>4</sup>Friedrich Schiller University Jena, Department of Geography, Jena, Germany

<sup>5</sup>Michael Stifel Center Jena for Data-driven and Simulation Science, Jena, Germany

**Correspondence:** Milan Flach ([milan.flach@bgc-jena.mpg.de](mailto:milan.flach@bgc-jena.mpg.de))

**Abstract.** Combined droughts and heatwaves are among those compound extreme events that induce severe impacts on the terrestrial biosphere and human health. A record breaking hot and dry compound event hit western Russia in summer 2010 (Russian heatwave, RHW). Events of this kind are typically studied either from a hydrometeorological perspective, or with a focus on impacts in the terrestrial biosphere such as reductions of the terrestrial carbon storage. These different perspectives might not only require different strategies for event detection, but also change interpretations and impact assessment. To exemplify this issue, we revisit the RHW both from a biospheric and a hydrometeorological perspective. We consider several hydrometeorological and biospheric variables agnostically as inputs to a recently developed multivariate anomaly detection approach. Our analysis of biospheric variables reveals that the RHW was preceded by increased gross ecosystem production in spring that partly compensated the reduced summer production, but remained unconsidered in earlier impact oriented studies. We also find that the region of reduced summer ecosystem production does not match the area identified as extreme in the hydrometeorological variables. The reason is that forest-dominated ecosystems in the higher latitudes respond with unusually high productivity to the RHW, leading overall to a compensation of 54% (36% in spring, 18% in summer) of the reduced gross primary production (GPP) in southern agriculturally dominated ecosystems. Our results show that an ecosystem-specific and multivariate perspective on extreme events can reveal multiple facets of extreme events by simultaneously integrating several data streams irrespective of impact direction and the variables' domain (here "biosphere" or "hydrometeorology"). Focusing on negative impacts in specific variables e.g. a vegetation index, leads to a spatiotemporally delineation of extreme events that is inconsistent with the hydrometeorological conditions and can limit the interpretation of their impacts on the terrestrial biosphere. Our study exemplifies the need for robust multivariate analytic approaches to detect extreme events in both hydrometeorological conditions and associated biosphere responses to fully characterize the effects of extremes, including possible compensatory effects in space and time.

**Keywords.** compound events, multivariate extreme events, gross primary productivity, heatwaves, droughts, spring-summer compensation.



## 1 Introduction

One consequence of global climate change is that the intensity and frequency of heatwaves will most likely be increasing in the coming decades (Seneviratne et al., 2012). Heatwaves co-occurring with droughts form so-called compound events, for which we can expect severe impacts on the functioning of land ecosystems (e.g. primary production, von Buttlar et al., 2018) that may affect human well-being (e.g. via reduced crop yields, health impacts) (e.g., Scheffran et al., 2012; Reichstein et al., 2013; Lesk et al., 2016). Investigating historical extreme events offers important insights for deriving mitigation strategies in the future.

One well-known example of a compound extreme event is the 2010 western Russian heatwave (RHW). The RHW was one of the most severe heatwaves on record, probably breaking temperature records of several centuries (Barriopedro et al., 2011). It was accompanied by extensive wild and peat fires with smoke plumes about 1.6 km high at the peak of the heatwave in early August, and estimated emissions of around 77 Tg carbon due to multiple fire events (Guo et al., 2017). Carbon losses due to reduced vegetation activity are estimated to be in the same order of magnitude as losses due to fires (90Tg, Bastos et al., 2014). The amount of emitted carbon monoxide is almost comparable to the anthropogenic emissions in this region (Konovalov et al., 2011). Approximately 55,000 cases of death have been attributed to health impacts of the RHW (Barriopedro et al., 2011).

The RHW is often associated with a atmospheric blocking situation (Matsueda, 2011), leading to a persistent anticyclonic weather pattern in Eastern Europe (Dole et al., 2011; Petoukhov et al., 2013; Schubert et al., 2014; Kornhuber et al., 2016).

However, to fully understand the developments and impacts of heatwaves or droughts, apart from hydrometeorological drivers, associated land-surface dynamics and feedbacks need to be considered (Seneviratne et al., 2010). For instance, under persistent anticyclonic and dry conditions, land-atmosphere feedbacks are expected to further amplify the magnitude of heatwaves via enhanced sensible heat fluxes, as shown also for the RHW (Miralles et al., 2014; Hauser et al., 2016). These feedback mechanisms highlight the importance of depleted soil moisture to heatwaves. In 2010 the depleted state of soil moisture was one important driver which locally amplified the high temperature regime (Hauser et al., 2016). It is a general observation that the combination of anticyclonic weather regimes and initially dry conditions prior to the event amplifies heatwaves in most cases (Quesada et al., 2012).

The direct impacts of such extreme events on ecosystems are manifold. Summer heat and drought typically reduce (or even inhibit) photosynthesis, hence reducing the carbon uptake potential of ecosystems (Reichstein et al., 2013). However, the magnitude of these impacts varies between ecosystems (Frank et al., 2015), and the resulting net effects are still under debate, particularly for heatwaves (von Buttlar et al., 2018). However, in-depth investigations of a number of individual events such as the European heat summer 2003 (Ciais et al., 2005), the 2000-2004 and 2012 droughts in North America (Schwalm et al., 2012; Wolf et al., 2016), and the RHW (Bastos et al., 2014) agree on an overall tendency towards negative impacts on the carbon accumulation potential.

The RHW has been thoroughly investigated from an hydrometeorological point of view linking the atmospheric blocking to the large-scale positive anomalies in air temperatures and negative anomalies in water availability (e.g., Barriopedro et al., 2011; Rahmstorf and Coumou, 2011). The event has been also well investigated with an emphasis on the biospheric impacts



describing the negative anomalies in ecosystem productivity and related vegetation indices (e.g., Bastos et al., 2014). However, investigating the two domains in isolation might lead to an inconsistent description and thus interpretation of what is thought to represent the very same extreme event. If we only look at the zonal evolution of the RHW (Fig. 1), we find that the spatiotemporal patterns of the temperature anomaly does not match the zonal anomaly in vegetation productivity anomalies. The figure reveals an unusually warm period during spring and one longer heatwave during summertime (Fig. 1a). Temperature anomalies exceeded more than 10 K in both spring and summer, while negative anomalies in gross primary productivity (GPP) occurred only in areas south of  $55^{\circ}N$  (Fig. 1c). Comparing these two Hovmöller diagrams shows that (1) the affected latitudinal range of the negative GPP anomaly is much smaller than the positive temperature anomaly and (2) one may easily overlook the positive GPP anomaly during spring that coincides with an anomalous warm state.

The inconsistency of spatiotemporal anomalies in the hydrometeorological conditions and biosphere responses during the RHW reflects different disciplinary perspectives. We suspect that this domain-specific point of view might become an issue in studies of this kind. The objective of this paper is therefore to revisit the RHW and to investigate differences in the description and consequent interpretation of the very same extreme event, when adopting a biospheric vs. hydrometeorological point of view. Moving from a compartment-specific perspective towards an integrated one requires a shift in the methodological focus.

Here, we use a multivariate extreme event detection approach that (1) does not differentiate between a positive and a negative extreme event, and (2) can equally be applied on any set of time series, regardless of whether they describe the biospheric or the hydrometeorological domain. We expect that we can reveal previously overlooked facets in the RHW and discuss whether an impact-agnostic approach as presented here may complement compartmental/domain approaches facilitating a broader perspective and improved interpretation of extreme events and their impacts.

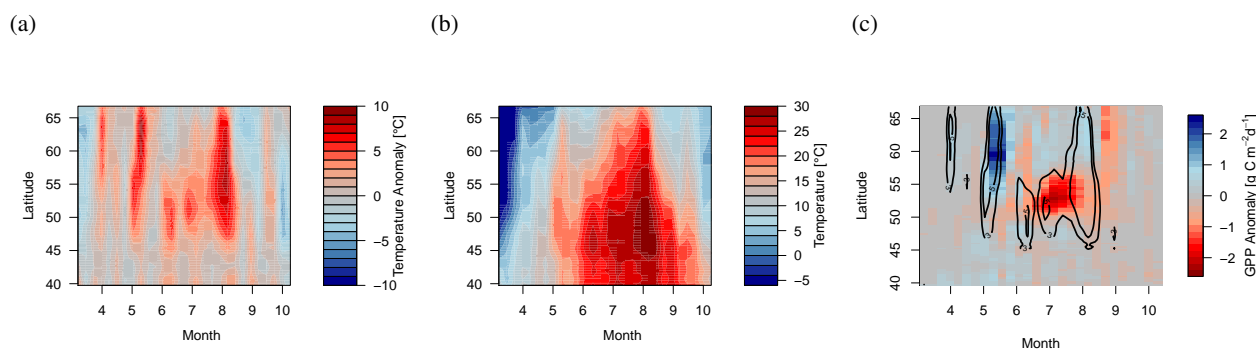


**Figure 1.** Longitudinal average ( $30.25$  to  $60.0^{\circ}E$ ) of (a) temperature anomalies, (b) absolute temperature, and (c) GPP anomalies in 2010 with a contour of temperature anomalies (+3 K, +5 K).

## 20 2 Methods & data

A simple approach to detect extreme events like the RHW could be using a peak-over-threshold scheme in the marginal distribution of variables of interest. For instance, a popular approach is to consider an observation in a single (ideally normally



distributed) anomaly variable to be extreme if it deviates by more than two standard deviations from the variable's mean values. By using these kind of univariate approaches for hydrometeorological variables, the RHW can be characterized by extremely high temperature anomalies, lack of precipitation and very low soil moisture, which amplified the heatwave (e.g., Miralles et al., 2014; Hauser et al., 2016). From this characterization it can be seen that more than one variable is involved in the RHW, which is thus a multivariate extreme event (i.e. a compound event) (e.g., Leonard et al., 2014; Zscheischler and Seneviratne, 2017). Multivariate algorithms to detect extreme events can therefore be expected to offer additional detection capabilities for simultaneous anomalies in multiple variables (e.g., Zimek et al., 2012; Bevacqua et al., 2017; Flach et al., 2017; Mahony and Cannon, 2018).

Multivariate extreme event detection methods account for dependencies and correlations among the selected variables. Multivariate extreme event detection considers all observable dimensions of the domain simultaneously. With a multivariate approach one may, for instance, detect very rare constellations of variables even if the individual variables are not extreme. In the following, we detect the anomalies in a multivariate variable space in two sets of variables describing (1) the hydrometeorological conditions, and (2) the biospheric response.

## 2.1 Data

Our dataset for analysing the hydrometeorological domain includes those variables which we consider to be of particular importance for processes taking place during extreme events in the biosphere based on prior process knowledge (Larcher, 2003) and empirical analysis (von Buttler et al., 2018). The hydrometeorological dataset consists of air temperature, radiation, relative humidity (all three from ERA-INTERIM, Dee et al., 2011), precipitation (Adler et al., 2003), and surface moisture (<http://www.gleam.eu>, v3.1a, Miralles et al., 2011; Martens et al., 2017). We consider surface moisture to be a hydrometeorological variable due to its importance for drought detection, although we notice that surface moisture is influenced by biospheric processes. We use gross primary productivity (GPP), latent heat flux (LE), sensible heat flux (H) (all three from FLUXCOM-RS, Tramontana et al., 2016), and the fraction of absorbed photosynthetic active radiation (FAPAR, moderate resolution imaging spectroradiometer (MODIS) based FAPAR, Myneni et al., 2002) to describe the land surface dynamics. We consider turbulent fluxes to be biospheric response variables because they are strongly determined by processes in the terrestrial biosphere.

The selected variables cover the spatial extent of Europe (latitude  $34.5 - 71.5^{\circ}N$ ; longitude:  $-18 - 60.5^{\circ}E$ ) and are re-gridded on a spatial resolution of  $0.25^{\circ}$  from 2001 to 2011 in an eight-daily temporal resolution. To check for differences in land cover types, we estimate the main land cover type of the European Space Agency Climate Change Initiative land cover classification on a spatial resolution  $0.25^{\circ}$ . To check for consistency of our findings among other variables (Sect. 3.2), we additionally use terrestrial ecosystem respiration (TER) and net ecosystem productivity (NEP, both originating from FLUXCOM-RS, Tramontana et al., 2016).



## 2.2 Preprocessing and spatiotemporal segmentation

For each variable under consideration, we compute a smoothed median seasonal cycle per grid cell to obtain an estimate of seasonality. We subtract the seasonal cycle from each variable and obtain a multivariate data cube of deviations from the median seasonality (Fig. 2, step 1). In this multivariate anomaly data cube, we fill small data gaps with zeros to ensure that they are not  
5 detected as anomalies.

To define extreme events in this multivariate data cube several approaches are possible. One approach would be to define thresholds globally. Spatiotemporal points exceeding the global threshold would be flagged as extreme event. However, the data is spatially heteroscedastic, i.e. a global approach detects extreme events in predominantly in high variance regions and is blind to regions with low variance. Another approach would be to define a certain threshold locally within each grid cell.  
10 This approach would assume an equal spatial distribution of extreme events which is particularly problematic for rather short time series as the ones under scrutiny. We use an alternative approach which compares grid cells to other grid cells with similar phenology recently developed by Mahecha et al. (2017) and extend it to the multivariate case by also including similar climatology. The regional approach is important in our case to get robust regional estimates of thresholds defining extreme events in rather short time series via spatial replicates. The main idea behind the scheme for identifying similar phenology and  
15 climate is that the principal components of the mean seasonal cycles and can be used for classifying regions according to their mean temporal dynamics.

The procedure for extracting spatial segments of similar grid cells works as follows (for a detailed description see Supplementary Materials S1 or Mahecha et al., 2017): (1) estimate the median seasonal cycle in each grid cell and of each variable individually and standardize the median seasonal cycles to zero mean and unit variance. Sort the median seasonal cycles ac-  
20 cording to the permutation of temperature to remove the effect of different phasing and concatenate the seasonal cycle of all variables. (2) Apply a principal component analysis to reduce the temporal dimension of the concatenated median seasonal cycles. (3) Select grid cells of similar phenology and climate by dividing the orthogonal principal component subspace into equally sized bins. The bins are sufficiently small compared to the length of the principal components to ensure a fine binning of very similar phenology and climate. (4) Select one grid cell and grid cells in their neighbouring bins to obtain overlapping  
25 spatial segments of similar phenology and climate.

After identifying similar regions one approach is to detect multivariate anomalies and define thresholds of the obtained anomaly scores in each of the spatially overlapping segments. However, the data also exhibits a changing variance within the year (temporal heteroscedasticity), the variance is e.g. higher during growing season in the set of biosphere variables. These heteroscedastic patterns lead to detecting extreme events predominantly during the high-variance season. To avoid these  
30 seasonal patterns in the extreme event detection scheme, we extract the season in a temporally overlapping moving window (9 observations, 72 days) and compare it to the same season in other years in the same grid cell and to the same season in grid cells with similar climate and phenology. Within the spatiotemporal segmentation procedure, we ensure that the number of observations is at least 198 (9 time steps  $\times$  11 years, at least one spatial replicate). We run the following anomaly detection workflow in each segment (Fig. 2, step 2).

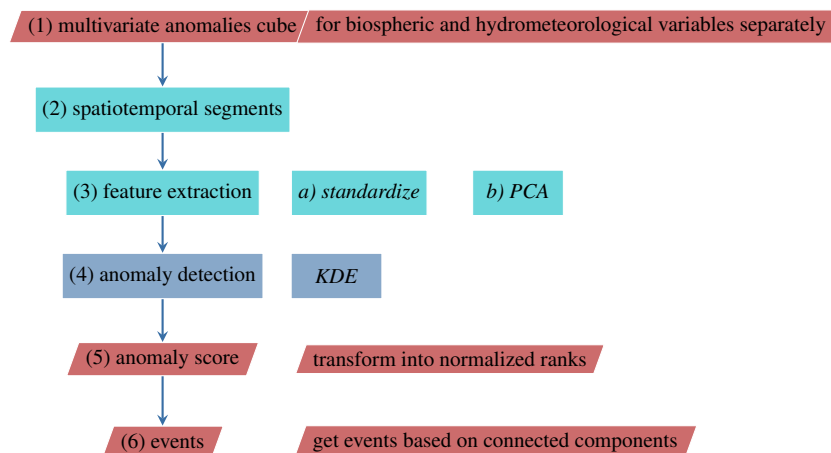


**Figure 2.** Data processing for detecting multivariate anomalies.

### 2.3 Feature extraction and anomaly detection

We apply the multivariate anomaly detection algorithm separately to the set of variables representing the biosphere and the hydrometeorology with a workflow proposed by Flach et al. (2017). In each spatiotemporal segment of the multivariate anomaly data cube we standardize the data to zero mean and unit variance (Fig. 2, step 3a). Subsequently, we calculate principal components (von Storch and Zwiers, 2001) of the variables in each spatiotemporal segment, thus representing the variables by orthogonal transformed vectors and retaining a number of principal components that explain more than 95% of the variance of this spatial segment (Fig. 2, step 3b). This procedure accounts for linear correlations in the data only and removes "unimportant" high dimensionality.

We choose kernel density estimation (KDE, Parzen, 1962; Harmeling et al., 2006) for multivariate extreme event detection in feature space (Fig. 2, step 4). KDE showed very good performance among different other options to detect multivariate anomalies in previous experiments (Flach et al., 2017). It considers nonlinear dependencies among principal components to obtain an anomaly score (Fig. 3). The anomaly scores are transformed into normalized ranks between 1.0 (very anomalous, data point in the margins of the multivariate distribution) and 0.0 (completely normal, data point in the dense region of the multivariate distribution) in each overlapping spatiotemporal segment (Fig. 2, step 5). To reunify the spatiotemporal segments, we assign the normalized anomaly scores temporally to the time step in the center of the temporal moving window and spatially to the grid cell in the central bin of similar climate and phenology.

### 2.4 Statistics of extreme events

We assume that 5% of the data are anomalous in each overlapping spatiotemporal segment and convert the anomaly scores into binary information. To compute statistics based on the spatiotemporal structure of each extreme event, we follow an approach developed by Lloyd-Hughes (2011); Zscheischler et al. (2013) and compute the connections between spatiotemporal extremes

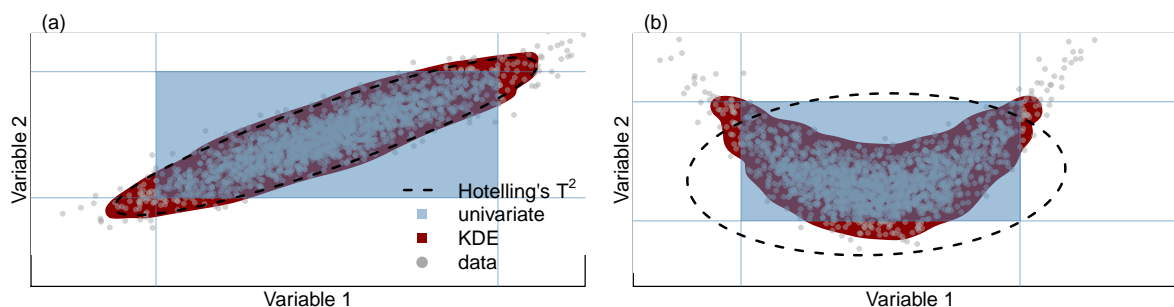


**Figure 3.** Illustration of the multivariate anomaly detection algorithm with two variables. The data has: (a) linear dependencies (multivariate normal) and (b) a nonlinear dependency structure. Univariate extreme event detection does not follow the shape of the data, whereas algorithms assuming a multivariate normal distribution (Hotelling's  $T^2$ , Lowry and Woodall, 1992) are suitable for case (a); kernel density estimation (KDE) gets the shape of the data in both cases (a) and (b). 5% extreme anomalies are outside the shaded areas (region of "normality") for all three algorithms.

if they are connected within a  $3 \times 3 \times 3$  (lon  $\times$  lat  $\times$  time) cube. Each connected anomaly is considered as a single event (Fig. 2, step 6). In this way, we observe event-based statistics, i.e. affected area ( $\text{km}^2$ ), affected volume ( $\text{km}^2 \cdot \text{days}$ ), centroids of the area and histograms of the single variable anomalies stratified according to different ecosystem types (land cover classes). Furthermore, we observe the response of individual variables to the multivariate event by computing the area weighted sum of the variable during the event in which the variable of interest is positive relative to the seasonal cycle ( $res^+$ ) or negative, respectively ( $res^-$ ). For many biospheric variables, one expects a mainly negative response to hydrometeorological extreme events like heatwaves or droughts (Larcher, 2003; von Buttler et al., 2018). Thus, we define compensation of a specific variable to be the absolute fraction of  $res^+$  from  $res^-$ . The balance of a variable is the sum of  $res^+$  and  $res^-$ . Centroids of  $res^+$  and  $res^-$  are computed as average of the affected longitudes, latitudes, and time period, weighted with the number of affected grid cells at this longitude, latitudes, and time period, and its respective anomaly score. They are to compute the spatial and temporal distance between  $res^+$  and  $res^-$ . Affected area, volume, response and centroids take the spherical geometry of the Earth into account by weighting the affected grid cells with the cosine of the respective latitude.

### 3 Results

#### 3.1 Extreme events in western Russia in 2010

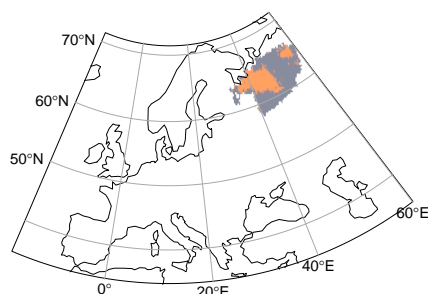
We identify two multivariate extreme events in the set of hydrometeorological variables in western Russia 2010, based on the spatiotemporal connectivity (more details Supplementary Materials S2). The two extreme events are separated by approximately one week of normal conditions towards the end of May:

- hydrometeorological spring event: anomaly of the hydrometeorological variables in western Russia during May ranging from longitude  $30.25 - 60.0^\circ \text{E}$ , latitude  $\geq 55^\circ \text{N}$  (Fig. 4a, b)

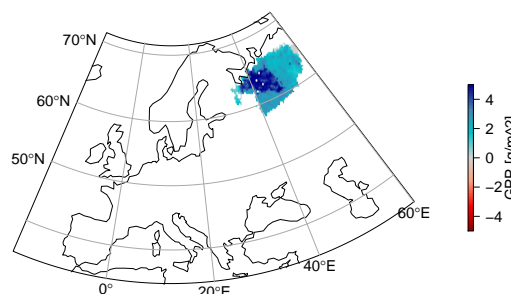




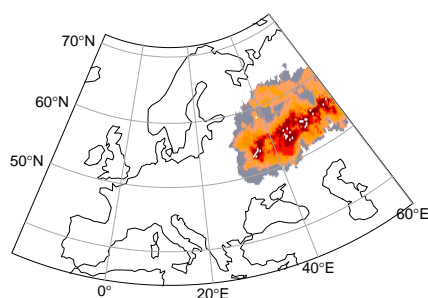
(a) duration of the hydrometeorological spring event



(b) sum of GPP during the hydrometeorological spring event



(c) duration of the hydrometeorological summer event



(d) sum of GPP during the hydrometeorological summer event

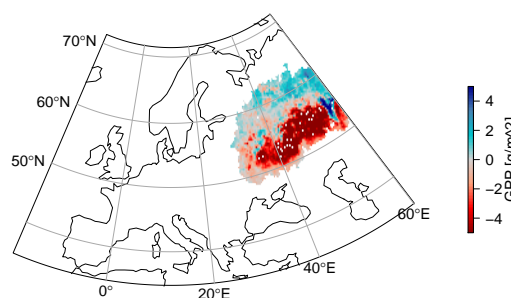


**Figure 4.** Left column: temporal duration of (a) the hydrometeorological spring event and (c) the hydrometeorological summer event. Right column: corresponding GPP response, i.e. the sum of deviations from the seasonal cycle during the event for (b) the hydrometeorological spring event and (d) the hydrometeorological summer event. While the GPP response during the hydrometeorological spring event is entirely positive (more productive than usual, b), GPP response during the hydrometeorological summer event differs between higher latitudes ( $> 55^\circ N$ , short-lasting, positive) and lower latitudes (long-lasting, negative).

- hydrometeorological summer event: anomaly of the hydrometeorological variables in western Russia, June to August, ranging from longitude  $28.75 - 60.25^\circ E$ , latitude  $48.25 - 66.75^\circ N$ . This event is usually referred to as Russian Heatwave (RHW) 2010 (e.g., Barriopedro et al., 2011; Rahmstorf and Coumou, 2011) (Fig. 4c, d).

Both multivariate hydrometeorological anomalies partly overlap with a multivariate anomaly in the set of biosphere variables (biospheric spring event and biospheric summer event). Of specific interest is that the area affected by anomalous hydrometeorological summer conditions is remarkably larger than the one detectable in the biospheric variables (biospheric summer event,  $2.4 \cdot 10^6$  vs.  $1.1 \cdot 10^6$  km<sup>2</sup>, Tab. 1). This fact might already indicate that biosphere responses are more nuanced and do not simply follow the extent of the hydrometeorological anomaly. As indicated e.g. also by Smith (2011), a hydrometeorological extreme event does not necessarily imply an extreme response.





**Table 1.** Statistics of the extreme events, based on their spatiotemporal connected structure: affected area, affected volume, positive and negative GPP response to the event, compensation of the negative response (comp.), as well as average spatial and temporal distance between the parts of the events with positive and negative responses.

event	area [ $km^2$ ]	volume [ $km^2 \cdot days$ ]	GPP comp.	$res_{GPP}^+$	$res_{GPP}^-$	spatial [km]	temporal [d]
hydrometeorological							
spring	$0.77 \cdot 10^6$	$0.81 \cdot 10^7$	-	$17.8 Tg$	-		
summer	$2.44 \cdot 10^6$	$5.79 \cdot 10^7$	0.18	$8.8 Tg$	$-49.0 Tg$	499	-4
integrated	$3.29 \cdot 10^6$	$6.60 \cdot 10^7$	0.56	$26.6 Tg$	$-49.0 Tg$	452	-34
biospheric							
spring	$1.25 \cdot 10^6$	$1.48 \cdot 10^7$	117.04	$33.8 Tg$	$-0.3 Tg$	756	-16
summer	$1.06 \cdot 10^6$	$4.22 \cdot 10^7$	0.00	$0.4 Tg$	$-82.4 Tg$	962	50
integrated	$2.28 \cdot 10^6$	$5.70 \cdot 10^7$	0.41	$34.2 Tg$	$-82.7 Tg$	514	-56

As GPP is a key determinant of ecosystem–atmosphere carbon fluxes and well described, we focus on the gross primary productivity (GPP) response to the multivariate hydrometeorological anomaly: We find that the GPP response is entirely positive during the short-lasting hydrometeorological spring event (+17.8 Tg C, Tab. 1), while it is mainly negative during the summer (+8.8 Tg C,  $-49$  Tg C, Tab. 1). Nonetheless, 18% of the GPP summer losses during the RHW are instantaneously compensated by over-productive vegetation in the northern latitudes. If we estimate the integrated effect of summer and spring anomalies, another 36% of the carbon losses are compensated during spring in higher latitudes. Overall, we find that 54% of the negative GPP responses are compensated either because of the positive spring anomalies or across ecosystems during summer. These compensation effects reduce the negative carbon impact of integrated annual (spring and summer) hydrometeorological event from  $-49.0$  Tg C to  $-24$  Tg C in total (Tab. 1).

Moving the focus to the multivariate biosphere events (biospheric spring and biospheric summer event), which overlap with the hydrometeorological events, we find that GPP responses based on the biospheric spring event are almost entirely positive (+33.8 Tg C), and based on the biospheric summer event almost entirely negative ( $-82.6$  Tg C). In total, 41% of the summer carbon losses are compensated by an anomalously productive spring (56 days earlier) in the higher latitudes (514 km distance of the centroids, Tab. 1). To further examine these findings, we check for these kind of compensation effects among different variables and another GPP dataset in the following section. Note that the dataset of biosphere variables includes GPP itself. Computing the responses based on the extent of the biospheric event is nevertheless useful, as an extreme event in the biosphere variables is not exclusively restricted to extreme conditions in the hydrometeorological conditions (Smith, 2011).

### 3.2 Compensation in other data-sets and variables

The integrated (spring and summer) compensation effect in GPP is highly consistent among different variables. For instance NEP (excluding fire) shows this kind of compensation, but also FAPAR and LE (Tab. 2). Sensible heat flux, on the other hand, is high during the hydrometeorological summer event (biospheric summer event), as well as the hydrometeorological



**Table 2.** Compensation of negative responses to the western Russian events in 2010 based on the integrated biospheric or hydrometeorological events is consistent over different variables and data sets.

Variable	hydrometeorological events			biospheric events		
	$res^+$ [ $Tg$ ]	$res^-$ [ $Tg$ ]	Comp. [%]	$res^+$ [ $Tg$ ]	$res^-$ [ $Tg$ ]	Comp. [%]
NEP	17.53 $Tg$	-34.03 $Tg$	51.5	23.45 $Tg$	-48.49 $Tg$	48.4
LE	19.90 $Tg$	-53.97 $Tg$	36.9	16.34 $Tg$	-102.81 $Tg$	15.9
FAPAR	1.89	-4.03 $Tg$	47.0	2.52 $Tg$	-6.61 $Tg$	38.1
TER	18.97 $Tg$	-11.06 $Tg$	171.4	13.71 $Tg$	-23.43 $Tg$	58.5

(a) hydrometeorological spring event

(b) hydrometeorological summer event

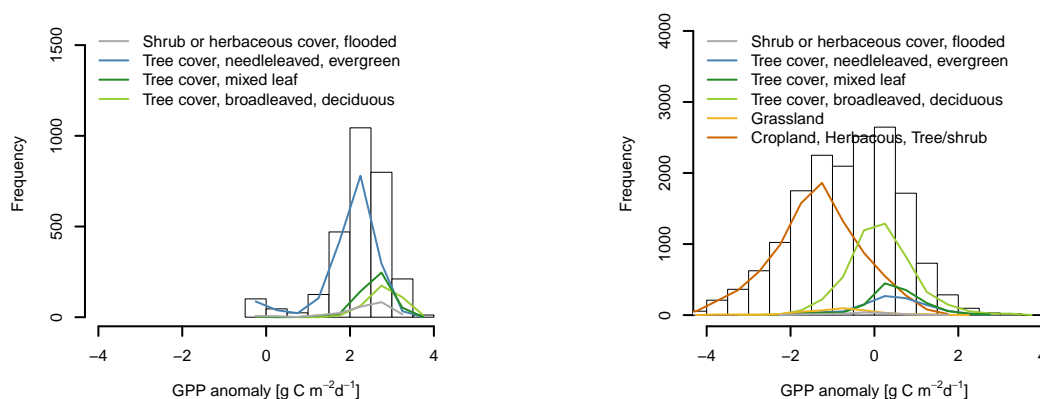


**Figure 5.** Histogram of GPP anomalies for different land cover classes based on the spatio-temporal extent of (a) the hydrometeorological spring event and (b) the hydrometeorological summer event. Bars denote the sum of all vegetation classes.

spring event (biospheric spring event) as expected for strong positive temperature anomalies. However, some of the remote sensing data products might be affected by high fire induced aerosol loadings during the heatwave that affect atmospheric optical thickness (e.g., Guo et al., 2017; Konovalov et al., 2011). Exploring an almost entirely climate-driven GPP product (FLUXCOM RS+METEO, Jung et al., 2017) also shows the integrated compensation effect, although much lesser pronounced (Appendix A1). Thus, we are confident that the observed compensation effect is not related to the optical thickness during the RHW.

### 3.3 Influence of Vegetation Types

In Fig. 5 we present the histograms of GPP anomalies for different land cover classes (forests, grasslands and crops) based on hydrometeorological spring event, hydrometeorological summer event, biospheric spring event, and biospheric summer event, respectively (Fig. B1) to highlight two aspects: First, during the spring event (hydrometeorological spring or biospheric

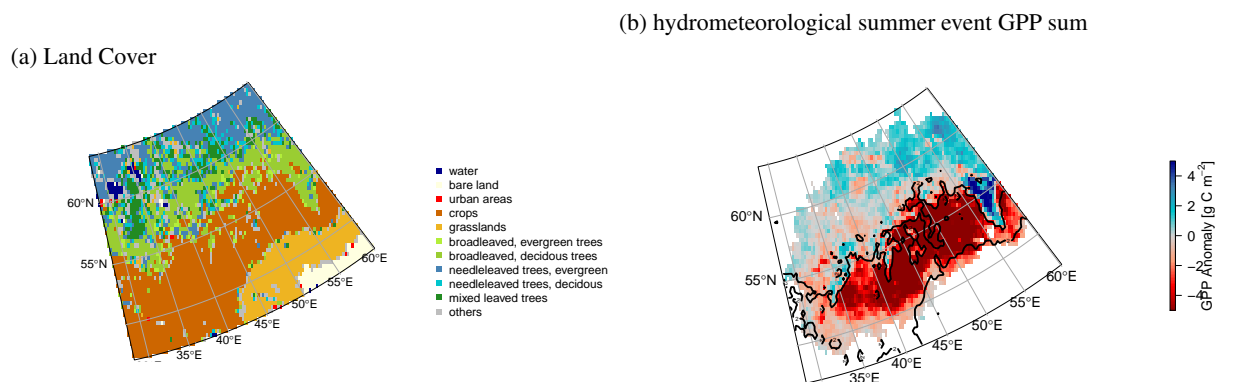


**Figure 6.** (a) Dominant land cover classes of a spatial extent of the RHW. (b) The boundaries of the different ecosystem types (forest-dominated ecosystems vs. agriculture-dominated ecosystems, denoted by the black contour line) match the observed patterns of the GPP response during the hydrometeorological summer event.

spring), forests react almost entirely with positive GPP anomalies (Fig. 5a). Thus, the timing of the extreme event (e.g. positive temperature anomalies in spring) leads to hydrometeorological conditions which are favourable for vegetation productivity, as absolute spring temperatures are still below the temperature optimum of GPP (Fig. 7a, Wolf et al., 2016; Wang et al., 2017).

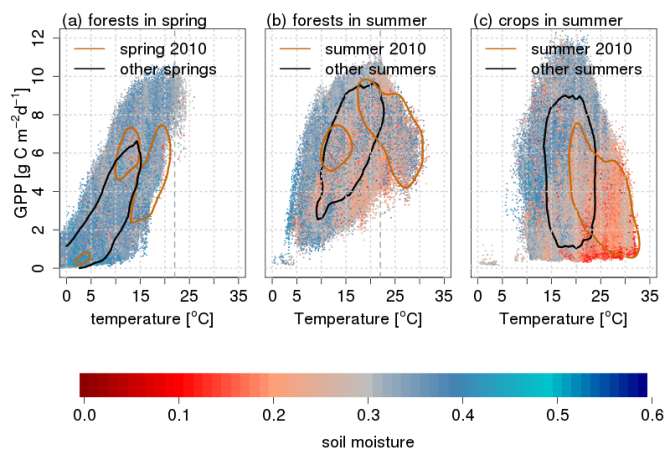


**Figure 7.** Temperature optimality for GPP in (a) forests during spring, (b) forests during summer, and (c) crops during summer. Contour lines enclose 75% of the data points.

Second, during the hydrometeorological summer event, we observe positive to neutral GPP responses in forests, whereas crops and grasslands react strongly negative (Fig. 5b). The positive versus negative GPP responses almost entirely reflect the map of dominant vegetation types (forest vs. agricultural ecosystems, Fig. 6). In fact, we can also show that from a statistical point of view vegetation type is the most important factor explaining the GPP response in summertime, followed by radiation



anomalies and duration (Supplementary S3). However, different vegetation types exhibit a transition from higher latitudes (predominantly forest ecosystems) to lower latitudes (dominated by agricultural ecosystems). Thus, the different responses of vegetation types might be confounded by the fact that absolute temperatures also follow a latitudinal gradient (Fig. 1b). Absolute temperatures for agricultural ecosystems are higher and far beyond the temperature optimum of GPP (7c), whereas forest-dominated ecosystems at higher latitudes experience temperatures just slightly above the temperature optimum of GPP (7b). The response of forest ecosystems partly reflects this kind of latitudinal gradient: forest ecosystems in the lower latitudes react positively to the spring temperature anomaly and then tend to react more negatively to the summer heatwave than forest ecosystems in higher latitudes. Forest ecosystems in higher latitudes are still productive in terms of GPP during the peak of the heatwave (Fig. 8). This finding is accompanied by consistently higher underlying water use efficiency (calculated according to Zhou et al. (2014) in forest-dominated ecosystems compared to agriculture-dominated ecosystems (Appendix Fig. C1a), and higher evaporative fraction in forest ecosystems during the peak of the heatwave (Appendix Fig. C1b).

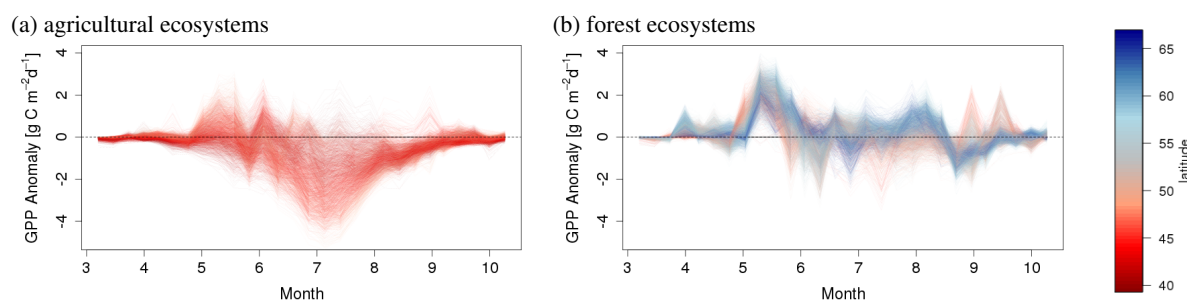


**Figure 8.** Temporal evolution of the GPP anomaly for (a) agricultural ecosystems and (b) forest ecosystems, colored according to the latitude.

#### 4 Discussion

In this paper we show that the hydrometeorological extreme events affecting western Russia in spring and summer 2010 do not fully correspond to the observed vegetation responses. Positive to neutral GPP responses prevail in higher latitudes during summer, whereas strong negative impacts on GPP can be found in lower latitudes. We interpret this effect by different water management strategies of forest vs. agricultural ecosystems (Teuling et al., 2010; van Heerwaarden and Teuling, 2014) that meet a general latitudinal temperature gradient. Apart from a more efficient water usage of forest-dominated ecosystems, access to deeper soil water might be another reason of ecosystem-specific responses (Fan et al., 2017; Yang et al., 2016). Note that the latitudinal temperature gradient alone might explain differences in the response within ecosystems in summer and between spring and summer, but does not sufficiently explain differentiated GPP responses in summer among different ecosystems (predominantly forest vs. agricultural ecosystems).

Compensations of carbon balance during hydrometeorological extreme events have been reported in earlier studies. For instance, Wolf et al. (2016) report that a warm spring season preceding the 2012 US summer drought reduced the impact on



the carbon cycle on the one side. Yet on the other side the increased spring productivity amplified the reduction in summer productivity by spring–summer carry-over effects via soil moisture depletion: higher spring productivity leads to higher water consumption in spring. The high water additionally consumed during spring reduces the water availability in summer and thereby affects productivity during the following summer. However, it remains unclear whether this observation was a singular case, or whether this compensation effect could become a characteristic pattern to be regularly expected in a warmer world. In this paper, we provide some evidence for presumed comparable compensation effects. In contrast to the discussion in Wolf et al. (2016), the RHW compensation does not exclusively occur temporally, i.e. spring compensating for summer losses, but rather spatially distinct forest ecosystems are identified as drivers for this compensation. Spatially compensating ecosystem effects to drought have been observed earlier in mountainous ecosystems that respond differently than lowlands during the European heatwave 2003 (Reichstein et al., 2007).

Following up on these compensation effects, Sippel et al. (2017) use ensemble model simulations to disentangle the contribution of spring compensation vs. spring carry-over effects on a larger scale. They show that warm springs increasingly compensate summer productivity losses in Europe, whereas spring–summer carry-over effects are constantly counteracting this compensation. We can confirm the general finding on spring compensation effects of summer productivity losses in observations for our case study on the RHW. Without using model simulations it is difficult to quantify spring–summer carry-over effects via soil moisture depletion. In case of the RHW only very few areas are anomalously productive in terms of GPP in spring and unproductive in summer as well. Thus, we suspect that exclusively temporal spring–summer carry-over effects play a rather small role for the RHW. However, we also emphasize that longer-term effects, such as compensation in subsequent year through species changes for instance (Wagg et al., 2017), have not been considered in the present study and likely remain hard to quantify beyond dedicated experiments

The RHW is probably among the best studied extreme events in the northern hemisphere. However, the compensation effects reported in this study have only received marginal attention so far. For instance, Wright et al. (2014) mention positive NDVI anomalies in spring 2010, but then focus largely on productivity losses in the Eurasian wheat belt. Similarly, Bastos et al. (2014) focus on a spatial extent of the biosphere impacts that only partly includes forest ecosystems at higher latitudes. Our estimation of carbon losses due to decreased vegetation activity (82 Tg C) is comparable to the one of Bastos et al. (2014) (90 Tg C). Similar to the results of our study, Yoshida et al. (2015) report reductions in photosynthetic activity in agriculture-dominated ecosystems during the RHW, but only small to no reductions in forest ecosystems during summertime. However, their interpretations focus on the summer heatwave. Nevertheless, re-evaluating impact maps (published e.g. in Wright et al., 2014; Yoshida et al., 2015; Zscheischler et al., 2015) in the light of our findings suggests that their evidence supports the presence of compensation effects during the RHW. When it comes to extreme events, the general tendency in many existing studies is naturally to focus on negative impacts as they are of particular interest for society (Bastos et al., 2014; Wright et al., 2014; Yoshida et al., 2015; Zscheischler et al., 2015). Thus, compensation effects remain unconsidered in previous studies on the RHW to the best of our knowledge.



## 5 Conclusions

We re-analysed biospheric and hydrometeorological conditions in western Russia 2010 with a generic spatiotemporal multivariate anomaly detection algorithm. We find that the hydrometeorological constellation and the biospheric responses exhibit two anomalous extreme events, one in late spring (May) and one over the entire summer (June, July, August), covering large areas of western Russia. For the summer event, we find that the spatially homogeneous anomaly pattern (characterized by high solar radiation and temperature, low relative humidity and precipitation) translate into a bimodal biosphere response. Forest ecosystems in higher latitudes show a positive anomaly in gross primary productivity, while agricultural systems decrease their productivity dramatically.

If we consider the integrated spring and summer effect of the anomalous hydrometeorological conditions, we find that forest ecosystems compensate for 54% (36% during spring, 18% during summer) of the productivity losses experienced in agricultural ecosystems. On the one hand, this finding highlights the importance of forest ecosystems to mitigate the impacts of climate extremes. On the other hand, however, this finding does not alleviate the consequences of extreme events for food security in agricultural ecosystems.

From a methodological point of view, this study emphasizes the importance of considering the multivariate nature of anomalies. From this study, we learn that it is insightful to consider both, the possibility of negative as well as of positive impacts, and assess their integrated compensation. Although the integrated impact on gross primary production of the hydrometeorological conditions is strongly negative, it is important to notice the strong compensatory effects due to differently affected ecosystem types, as well as duration and timing of the extreme events.



## Appendix A: Comparison with METEO + RS

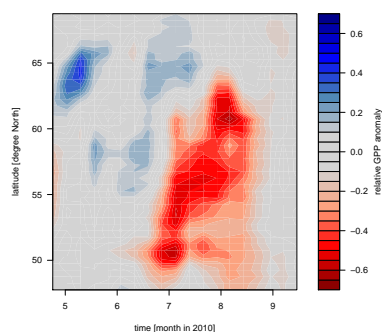
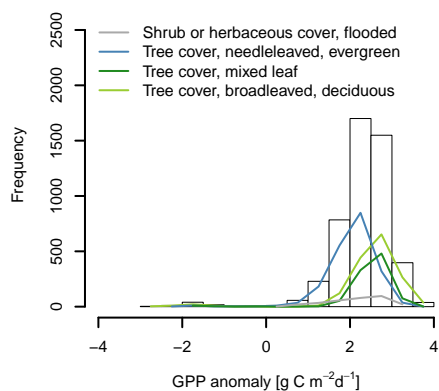


**Figure A1.** The longitudinal (30.25-60.25° E) average of the GPP anomalies during the RHW 2010, based on the Climate Research Unit observation-based climate variables (CRUNCEPv6, New et al., 2000) driven GPP product originating from FLUXCOM RS+METEO (Jung et al., 2017) shows similar but weaker compensation effects. 28% of the negative GPP response to the RHW are compensated based on the shown latitude-longitude subset.

## Appendix B: Biosphere response

(a) biospheric spring event



(b) biospheric summer event

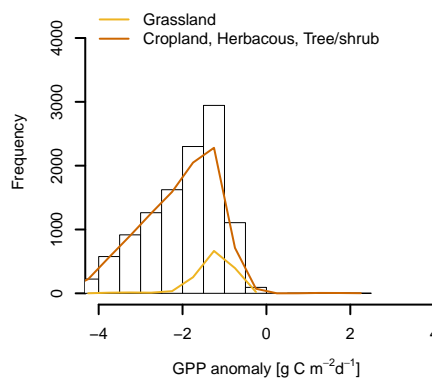
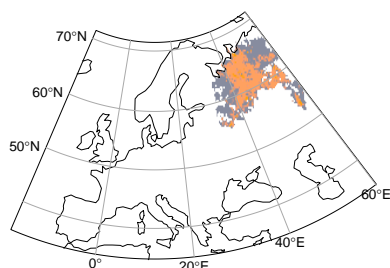


**Figure B1.** Histogram of GPP anomalies for different land cover classes constrained by a) biospheric spring and b) biospheric summer event.

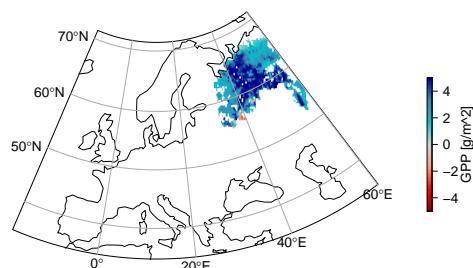




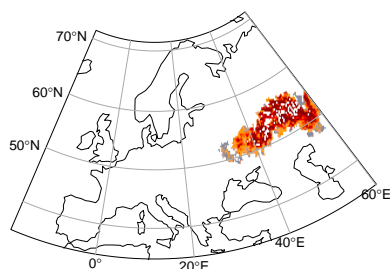
(a) biospheric spring event duration



(b) biospheric spring event GPP sum



(c) biospheric summer event duration



(d) biospheric summer event GPP sum

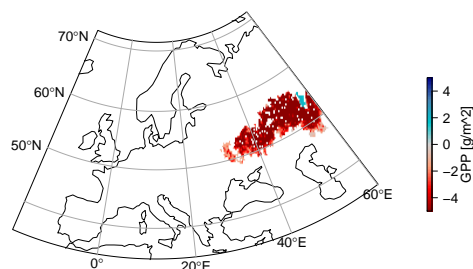
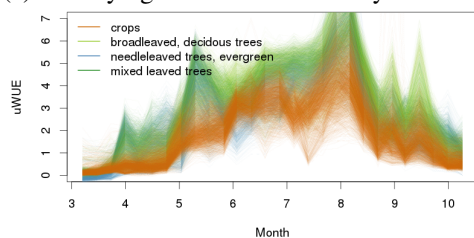


**Figure B2.** Left hand side: temporal duration of (a) biospheric spring, and (c) biospheric summer event. Right hand side: corresponding GPP response, i.e. the deviation from the seasonal cycle during the event for (b) biospheric spring, and (d) biospheric summer event. The Biospheric summer event is missing the positive response of forests at higher latitudes, as the response was positive, but is not considered to be "extremely" positive. Therefore, it is not detected by the multivariate algorithm.

### Appendix C: Water use efficiency and evaporative fraction of different land cover types

(a) underlying Water Use Efficiency



(b) Evaporative Fraction

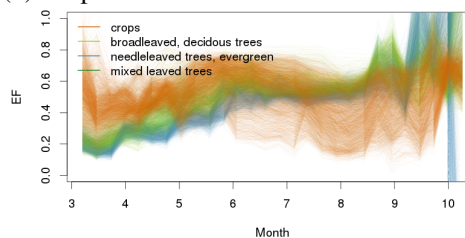


**Figure C1.** (a) Underlying water use efficiency (uWUE) and (b) evaporative fraction (EF) of the area affected by the RHW in 2010. uWUE is calculated according to Zhou et al. (2014) including vapour pressure deficit. In contrast to WUE, uWUE attempts to correct for differences in temperature and vapour pressure deficit to a certain degree.



*Author contributions.* MF and MDM designed the study in collaboration with SS, FG, ABa, ABr and MR. MF conducted the analysis and wrote the manuscript with contributions from all co-authors.

*Competing interests.* The authors declare that they have no conflict of interest.

*Acknowledgements.* This research received funding by the European Space Agency (project "Earth System Data Lab") and the European Union's Horizon 2020 research and innovation programme (project "BACI", grant agreement no 64176). The authors are grateful to the FLUXCOM initiative (<http://www.fluxcom.org>) for providing the data. MF acknowledges support by the International Max Planck Research School for Global Biogeochemical Cycles (IMPRS). Furthermore, the authors would like to thank Sebastian Bathiany for crucial discussions on the topic, Jürgen Knauer for his expertise on water use efficiency, Julia Kiefer for her kind language check, as well as Victor Brovkin and Sophia Walther helping to improve the manuscript.



## References

- Adler, R. F., Huffman, G. F., Chang, A., Ferraro, R., Xie, P.-P., Janowiak, J., Rudolf, B., Schneider, U., Curtis, S., Bolvins, D., Gruber, A., Susskind, J., Arkin, P., and Nelkin, E.: The Version-2 Global Precipitation Climatology Project (GPCP) Monthly Precipitation Analysis (1979–Present), *Journal of Hydrometeorology*, 4, 1147–1167, 2003.
- 5 Barriopedro, D., Fischer, E. M., Luterbacher, J., Trigo, R. M., and Garcia-Herrera, R.: The Hot Summer of 2010: Redrawing the Temperature Record Map of Europe, *Science*, 332, 220–224, 2011.
- Bastos, A., Gouveia, C. M., Trigo, R. M., and Running, S. W.: Analysing the spatio-temporal impacts of the 2003 and 2010 extreme heatwaves on plant productivity in Europe, *Biogeosciences*, 11, 3421–3435, 2014.
- Bevacqua, E., Maraun, D., Hobæk Haff, I., Widmann, M., and Vrac, M.: Multivariate statistical modelling of compound events via pair-copula constructions: analysis of floods in Ravenna (Italy), *Hydrology and Earth System Sciences*, 21, 2701–2723, 2017.
- 10 Ciais, P., Reichstein, M., Viovy, N., Granier, A., Ogée, J., Allard, V., Aubinet, M., Buchmann, N., Bernhofer, C., Carrara, A., Chevallier, F., De Noblet, N., Friend, A. D., Friedlingstein, P., Grünwald, T., Heinesch, B., Keronen, P., Knohl, A., Krinner, G., Loustau, D., Manca, G., Matteucci, G., Miglietta, F., Ourcival, J. M., Papale, D., Pilegaard, K., Rambal, S., Seufert, G., Soussana, J. F., Sanz, M. J., Schulze, E. D., Vesala, T., and Valentini, R.: Europe-wide reduction in primary productivity caused by the heat and drought in 2003, *Nature*, 437, 529–533, 2005.
- 15 Dee, D. P., Uppala, S. M., Simmons, A. J., Berrisford, P., Poli, P., Kobayashi, S., Andrae, U., Balmaseda, M. A., Balsamo, G., Bauer, P., Bechtold, P., Beljaars, A. C. M., van de Berg, L., Bidlot, J., Bormann, N., Delsol, C., Dragani, R., Fuentes, M., Geer, A. J., Haimberger, L., Healy, S. B., Hersbach, H., Hólm, E. V., Isaksen, I., Kållberg, P., Köhler, M., Matricardi, M., McNally, A. P., Monge-Sanz, B. M., Morcrette, J. J., Park, B. K., Peubey, C., de Rosnay, P., Tavolato, C., Thépaut, J. N., and Vitart, F.: The ERA-Interim reanalysis: configuration and performance of the data assimilation system, *Quarterly Journal of the Royal Meteorological Society*, 137, 553–597, 2011.
- 20 Dole, R., Hoerling, M., Perlwitz, J., Eischeid, J., Pegion, P., Zhang, T., Quan, X.-W., Xu, T., and Murray, D.: Was there a basis for anticipating the 2010 Russian heat wave?, *Geophys. Res. Lett.*, 38, L06702, 2011.
- Fan, Y., Miguez-Macho, G., Jobbágy, E. G., Jackson, R. B., and Otero-Casal, C.: Hydrologic regulation of plant rooting depth, *Proceedings of the National Academy of Sciences*, 82, 201712381, 2017.
- 25 Flach, M., Gans, F., Brenning, A., Denzler, J., Reichstein, M., Rodner, E., Bathiany, S., Bodesheim, P., Guaniche, Y., Sippel, S., and Mahecha, M. D.: Multivariate anomaly detection for Earth observations: a comparison of algorithms and feature extraction techniques, *Earth System Dynamics*, 8, 677–696, 2017.
- Frank, D., Reichstein, M., Bahn, M., Thonicke, K., Frank, D., Mahecha, M. D., Smith, P., van der Velde, M., Vicca, S., Babst, F., Beer, C., Buchmann, N., Canadell, J. G., Ciais, P., Cramer, W., Ibrom, A., Miglietta, F., Poulter, B., Rammig, A., Seneviratne, S. I., Walz, A., Wattenbach, M., Zavala, M. A., and Zscheischler, J.: Effects of climate extremes on the terrestrial carbon cycle: concepts, processes and potential future impacts, *Global Change Biology*, 21, 2861–2880, 2015.
- 30 Guo, M., Li, J., Xu, J., Wang, X., He, H., and Wu, L.: CO<sub>2</sub> emissions from the 2010 Russian wildfires using GOSAT data, *Environmental Pollution*, 226, 60–68, 2017.
- Harmeling, S., Dornhege, G., Tax, D., Meinecke, F., and Müller, K.-R.: From outliers to prototypes: Ordering data, *Neurocomputing*, 69, 1608–1618, 2006.
- 35 Hauser, M., Orth, R., and Seneviratne, S. I.: Role of soil moisture versus recent climate change for the 2010 heat wave in Russia, *Geophysical Research Letters*, 43, 2819–2826, 2016.



- Jung, M., Reichstein, M., Schwalm, C. R., Huntingford, C., Sitch, S., Ahlström, A., Arneth, A., Camps-Valls, G., Ciais, P., Friedlingstein, P., Gans, F., Ichii, K., Jain, A. K., Kato, E., Papale, D., Poulter, B., Ráduly, B., Rödenbeck, C., Tramontana, G., Viovy, N., Wang, Y.-P., Weber, U., Zaehle, S., and Zeng, N.: Compensatory water effects link yearly global land CO<sub>2</sub> sink changes to temperature, *Nature*, 541, 516–520, 2017.
- 5 Konovalov, I. B., Beekmann, M., Kuznetsova, I. N., Yurova, A., and Zvyagintsev, A. M.: Atmospheric impacts of the 2010 Russian wildfires: integrating modelling and measurements of an extreme air pollution episode in the Moscow region, *Atmos. Chem. Phys.*, 11, 10031–10056, 2011.
- Kornhuber, K., Petoukhov, V., Petri, S., Rahmstorf, S., and Coumou, D.: Evidence for wave resonance as a key mechanism for generating high-amplitude quasi-stationary waves in boreal summer, *Climate Dynamics*, 49, 1961–1979, 2016.
- 10 Larcher, W.: *Physiological plant ecology: ecophysiology and stress physiology of functional groups.*, Springer Science & Business Media, Berlin, 2003.
- Leonard, M., Westra, S., Phatak, A., Lambert, M., van den Hurk, B., McInnes, K., Risbey, J., Schuster, S., Jakob, D., and Stafford-Smith, M.: A compound event framework for understanding extreme impacts, *Wiley Interdisciplinary Reviews: Climate Change*, 5, 113–128, 2014.
- Lesk, C., Rowhani, P., and Ramankutty, N.: Influence of extreme weather disasters on global crop production, *Nature*, 529, 84–87, 2016.
- 15 Lloyd-Hughes, B.: A spatio-temporal structure-based approach to drought characterisation, *International Journal of Climatology*, 32, 406–418, 2011.
- Lowry, C. A. and Woodall, W. H.: A Multivariate Exponentially Weighted Moving Average Control Chart, *Technometrics*, 34, 46–53, 1992.
- Mahecha, M. D., Gans, F., Sippel, S., Donges, J. F., Kaminski, T., Metzger, S., Migliavacca, M., Papale, D., Rammig, A., and Zscheischler, J.: Detecting impacts of extreme events with ecological in situ monitoring networks, *Biogeosciences*, 14, 4255–4277, 2017.
- 20 Mahony, C. R. and Cannon, A. J.: Wetter summers can intensify departures from natural variability in a warming climate, *Nature Communications*, 9, 783, 2018.
- Martens, B., Miralles, D. G., Lievens, H., van der Schalie, R., de Jeu, R. A. M., Fernández-Prieto, D., Beck, H. E., Dorigo, W. A., and Verhoest, N. E. C.: GLEAM v3: satellite-based land evaporation and root-zone soil moisture, *Geoscientific Model Development*, 10, 1903–1925, 2017.
- 25 Matsueda, M.: Predictability of Euro-Russian blocking in summer of 2010, *Geophys. Res. Lett.*, 38, L06 801, 2011.
- Miralles, D. G., Holmes, T. R. H., De Jeu, R. A. M., Gash, J. H., Meesters, A. G. C. A., and Dolman, A. J.: Global land-surface evaporation estimated from satellite-based observations, *Hydrology and Earth System Sciences*, 15, 453–469, 2011.
- Miralles, D. G., Teuling, A. J., van Heerwaarden, C. C., and Vilà-Guerau de Arellano, J.: Mega-heatwave temperatures due to combined soil desiccation and atmospheric heat accumulation, *Nature Geoscience*, 7, 345–349, 2014.
- 30 Myneni, R. B., Hoffman, S., Knyazikhin, Y., Privette, J. L., Glassy, J., Tian, Y., Wang, Y., Song, X., Zhang, Y., Smith, G. R., Lotsch, A., Friedl, M. A., Morisette, J. T., Votava, P., Nemani, R. R., and Running, S. W.: Global products of vegetation leaf area and fraction absorbed PAR from year one of MODIS data, *Remote Sensing of Environment*, 83, 214–231, 2002.
- New, M., Hulme, M., and Jones, P.: Representing Twentieth-Century Space–Time Climate Variability. Part II: Development of 1901–96 Monthly Grids of Terrestrial Surface Climate, *Journal of Climate*, 13, 2217–2238, 2000.
- 35 Parzen, E.: On Estimation of a Probability Density Function and Mode, *The Annals of Mathematical Statistics*, 33, 1065–1076, 1962.
- Petoukhov, V., Rahmstorf, S., Petri, S., and Schellnhuber, H.-J.: Quasiresonant amplification of planetary waves and recent Northern Hemisphere weather extremes, *PNAS*, 110, 5336–5341, 2013.



- Quesada, B., Vautard, R., Yiou, P., Hirschi, M., and Seneviratne, S. I.: Asymmetric European summer heat predictability from wet and dry southern winters and springs, *Nature Climate Change*, 2, 736–741, 2012.
- Rahmstorf, S. and Coumou, D.: Increase of extreme events in a warming world, *PNAS*, 108, 17 905–17 909, 2011.
- Reichstein, M., Ciais, P., Papale, D., Valentini, R., Running, S., Viovy, N., Cramer, W., Granier, A., Ogée, J., Allard, V., Aubinet, M., Bernhofer, C., Buchmann, N., Carrara, A., Grünwald, T., Heimann, M., Heinesch, B., Knohl, A., Kutsch, W., Loustau, D., Manca, G., Matteucci, G., Miglietta, F., Ourcival, J.-M., Pilegaard, K., Pumpanen, J., Rambal, S., Schaphoff, S., Seufert, G., Soussana, J. F., Sanz, M. J., Vesala, T., and Zhao, M.: Reduction of ecosystem productivity and respiration during the European summer 2003 climate anomaly: a joint flux tower, remote sensing and modelling analysis, *Global Change Biology*, 13, 634–651, 2007.
- Reichstein, M., Bahn, M., Ciais, P., Frank, D., Mahecha, M. D., Seneviratne, S. I., Zscheischler, J., Beer, C., Buchmann, N., Frank, D. C., Papale, D., Rammig, A., Smith, P., Thonicke, K., van der Velde, M., Vicca, S., Walz, A., and Wattenbach, M.: Climate extremes and the carbon cycle, *Nature*, 500, 287–295, 2013.
- Scheffran, J., Brzoska, M., Kominek, J., Link, P. M., and Schilling, J.: Climate Change and Violent Conflict, *Science*, 336, 869–871, 2012.
- Schubert, S. D., Wang, H., Koster, R. D., Suarez, M. J., and Groisman, P. Y.: Northern Eurasian Heat Waves and Droughts, *Journal of Climate*, 27, 3169–3207, 2014.
- Schwalm, C. R., Williams, C. A., Schaefer, K., Baldocchi, D., Black, T. A., Goldstein, A. H., Law, B. E., Oechel, W. C., U, K. T. P., and Scott, R. L.: Reduction in carbon uptake during turn of the century drought in western North America, *Nature Geoscience*, 5, 551–556, 2012.
- Seneviratne, S. I., Corti, T., Davin, E. L., Hirschi, M., Jaeger, E. B., Lehner, I., Orlowsky, B., and Teuling, A. J.: Investigating soil moisture–climate interactions in a changing climate: A review, *Earth Science Reviews*, 99, 125–161, 2010.
- Seneviratne, S. I., Nicholls, N., Easterling, D., Goodess, C., Kanae, S., Kossin, J., Luo, Y., Marengo, J., McInnes, K., Rahimi, M., Reichstein, M., Sorteberg, A., Vera, C., and Zhang, X.: Changes in climate extremes and their impacts on the natural physical environment, in: *Managing the Risks of Extreme Events and Disasters to Advance Climate Change Adaptation (IPCC SREX Report)*, edited by Field, C., Barros, V., Stocker, T., Qin, D., Dokken, D., Ebi, K., Mastrandrea, M., Mach, K., Plattner, G.-K., Allen, S., Tignor, M., and Midgley, pp. 109–230, Cambridge University Press, 2012.
- Sippel, S., Forkel, M., Rammig, A., Thonicke, K., Flach, M., Heimann, M., Otto, F. E. L., Reichstein, M., and Mahecha, M. D.: Contrasting and interacting changes in simulated spring and summer carbon cycle extremes in European ecosystems, *Environ. Res. Lett.*, 12, 075 006, 2017.
- Smith, M. D.: An ecological perspective on extreme climatic events: a synthetic definition and framework to guide future research, *Journal of Ecology*, 99, 656–663, 2011.
- Teuling, A. J., Seneviratne, S. I., Stöckli, R., Reichstein, M., Moors, E. J., Ciais, P., Luyssaert, S., van den Hurk, B., Ammann, C., Bernhofer, C., Dellwik, E., Gianelle, D., Gielen, B., Grünwald, T., Klumpp, K., Montagnani, L., Moureaux, C., Sottocornola, M., and Wohlfahrt, G.: Contrasting response of European forest and grassland energy exchange to heatwaves, *Nature Geoscience*, 3, 722–727, 2010.
- Tramontana, G., Jung, M., Schwalm, C. R., Ichii, K., Camps-Valls, G., Ráduly, B., Reichstein, M., Arain, M. A., Cescatti, A., Kiely, G., Merbold, L., Serrano-Ortiz, P., Sickert, S., Wolf, S., and Papale, D.: Predicting carbon dioxide and energy fluxes across global FLUXNET sites with regression algorithms, *Biogeosciences*, 13, 4291–4313, 2016.
- van Heerwaarden, C. C. and Teuling, A. J.: Disentangling the response of forest and grassland energy exchange to heatwaves under idealized land–atmosphere coupling, *Biogeosciences*, 11, 6159–6171, 2014.



- von Buttlar, J., Zscheischler, J., Rammig, A., Sippel, S., Reichstein, M., Knohl, A., Jung, M., Menzer, O., Arain, M. A., Buchmann, N., Cescatti, A., Gianelle, D., Kiely, G., Law, B. E., Magliulo, V., Margolis, H., McCaughey, H., Merbold, L., Migliavacca, M., Montagnani, L., Oechel, W., Pavelka, M., Peichl, M., Rambal, S., Raschi, A., Scott, R. L., Vaccari, F. P., van Gorsel, E., Varlagin, A., Wohlfahrt, G., and Mahecha, M. D.: Impacts of droughts and extreme-temperature events on gross primary production and ecosystem respiration: a systematic assessment across ecosystems and climate zones, *Biogeosciences*, 15, 1293–1318, 2018.
- von Storch, H. and Zwiers, F. W.: *Statistical Analysis in Climate Research*, Cambridge Univ. Press, Cambridge, U. K., 2001.
- Wagg, C., O'Brien, M. J., Vogel, A., Scherer-Lorenzen, M., Eisenhauer, N., Schmid, B., and Weigelt, A.: Plant diversity maintains long-term ecosystem productivity under frequent drought by increasing short-term variation, *Ecology*, 98, 2952–2961, 2017.
- Wang, E., Martre, P., Zhao, Z., Ewert, F., Maiorano, A., Rötter, R. P., Kimball, B. A., Ottman, M. J., Wall, G. W., White, J. W., Reynolds, M. P., Alderman, P. D., Aggarwal, P. K., Anothai, J., Basso, B., Biernath, C., Cammarano, D., Challinor, A. J., De Sanctis, G., Doltra, J., Dumont, B., Fereres, E., Garcia-Vila, M., Gayler, S., Hoogenboom, G., Hunt, L. A., Izaurre, R. C., Jabloun, M., Jones, C. D., Kersebaum, K. C., Koehler, A.-K., Liu, L., Müller, C., Kumar, S. N., Nendel, C., O'Leary, G., Olesen, J. E., Palosuo, T., Priesack, E., Rezaei, E. E., Ripoche, D., Ruane, A. C., Semenov, M. A., Shcherbak, I., Stöckle, C., Stratonovitch, P., Streck, T., Supit, I., Tao, F., Thorburn, P., Waha, K., Wallach, D., Wang, Z., Wolf, J., Zhu, Y., and Asseng, S.: The uncertainty of crop yield projections is reduced by improved temperature response functions, *Nature Plants*, 3, 17102, 2017.
- Wolf, S., Keenan, T. F., Fisher, J. B., Baldocchi, D. D., Desai, A. R., Richardson, A. D., Scott, R. L., Law, B. E., Litvak, M. E., Brunsell, N. A., Peters, W., and van der Laan-Luijkx, I. T.: Warm spring reduced carbon cycle impact of the 2012 US summer drought, *Proceedings of the National Academy of Sciences*, 113, 5880–5885, 2016.
- Wright, C. K., de Beurs, K. M., and Henebry, G. M.: Land surface anomalies preceding the 2010 Russian heat wave and a link to the North Atlantic oscillation, *Environ. Res. Lett.*, 9, 124015, 2014.
- Yang, Y., Donohue, R. J., and McVicar, T. R.: Global estimation of effective plant rooting depth: Implications for hydrological modeling, *Water Resources Research*, 52, 8260–8276, 2016.
- Yoshida, Y., Joiner, J., Tucker, C., Berry, J., Lee, J. E., Walker, G., Reichle, R., Koster, R., Lyapustin, A., and Wang, Y.: The 2010 Russian drought impact on satellite measurements of solar-induced chlorophyll fluorescence: Insights from modeling and comparisons with parameters derived from satellite reflectances, *Remote Sensing of Environment*, 166, 163–177, 2015.
- Zhou, S., Yu, B., Huang, Y., and Wang, G.: The effect of vapor pressure deficit on water use efficiency at the subdaily time scale, *Geophys. Res. Lett.*, 41, 5005–5013, 2014.
- Zimek, A., Schubert, E., and Kriegel, H.-P.: A survey on unsupervised outlier detection in high-dimensional numerical data, *Statistical Analysis and Data Mining*, 5, 363–387, 2012.
- Zscheischler, J. and Seneviratne, S. I.: Dependence of drivers affects risks associated with compound events, *Science Advances*, 3, e1700263, 2017.
- Zscheischler, J., Mahecha, M. D., Harmeling, S., and Reichstein, M.: Detection and attribution of large spatiotemporal extreme events in Earth observation data, *Ecological Informatics*, 15, 66–73, 2013.
- Zscheischler, J., Orth, R., and Seneviratne, S. I.: A submonthly database for detecting changes in vegetation-atmosphere coupling, *Geophys. Res. Lett.*, 42, 9816–9824, 2015.